

## MEASURING TEMPORAL PHOTON BUNCHING IN BLACKBODY RADIATION

P. K. TAN<sup>1,2,\*</sup>, G. H. YEO<sup>2</sup>, H. S. POH<sup>1</sup>, A. H. CHAN<sup>2</sup>, AND C. KURTSIEFER<sup>1,2,+</sup>*Draft version March 31, 2014*

## ABSTRACT

Light from thermal black body radiators such as stars exhibits photon bunching behaviour at sufficiently short timescales. However, with available detector bandwidths, this bunching signal is difficult to be directly used for intensity interferometry with sufficient statistics in astronomy. Here we present an experimental technique to increase the photon bunching signal in blackbody radiation via spectral filtering of the light source. Our measurements reveal strong temporal photon bunching in light from blackbody radiation, including the Sun. Such filtering techniques may revive the interest in intensity interferometry as a tool in astronomy.

*Subject headings:* instrumentation: interferometers — radiation mechanism: thermal — stars: fundamental parameters — Sun: fundamental parameters — techniques: interferometric

## 1. BACKGROUND

Statistical intensity fluctuations from stationary thermal light sources formed the basis of the landmark experiments by Hanbury-Brown and Twiss (Hanbury-Brown & Twiss 1954, 1957), where correlation measurements between a pair of photodetection signals form a useful tool to assess both temporal and spatial coherence properties of light fields. The explanation for these fluctuations as photon bunching phenomenon, as compared to a Poissonian distribution for uncorrelated detection processes (Glauber 1963) was a major contribution for the development of the field of quantum optics.

Hanbury-Brown and Twiss developed their observation into a spatial intensity interferometer which allowed them to infer stellar angular radii from the coherence properties of star light over relatively large distances (Hanbury-Brown & Twiss 1956). Since a key quality of any telescope system is its angular resolution, given by its real or virtual aperture, they managed to carry out these measurements with an unprecedented accuracy.

While stellar amplitude interferometry has evolved to be a standard technique to increase the effective angular resolution of radio telescope arrays, the angular resolution of the Hanbury-Brown–Twiss approach is still unmatched by conventional diffraction-limited optical telescopes. It is also very challenging to reproduce with Michelson interferometry due to the required sub-wavelength optical path length stability. Such setups involve expensive and complicated orbital platforms or remote locations for observatory sites, and adaptive optics to augment the measurable sensitivity by suppressing optical noise (Millour 2008). Yet, the comparatively simple optical intensity interferometry technique has not really found widespread adoption in the observation of celestial objects.

## 2. THE PROBLEM

Temporal photon bunching, i.e., the tendency for photons to cluster together on a short time-scale, has been consistently observed from narrow-band quasi-thermal light sources such as halogen discharge lamps (Martienssen & Spiller 1964; Morgan & Mandel 1966) and laser beams (Asakura 1970) which passed through a rotating ground glass to randomize the optical phase in time.

Photon bunching in time for stationary fields is quantified by a second order correlation function  $g^{(2)}(\tau)$ , which is the probability of observing a second photodetection event a time  $\tau$  after a first one, normalized to the probability of an uncorrelated detection. Optical modes in thermal states are the textbook example where  $g^{(2)} = 2$  (Glauber 1963; Mandel & Wolf 1995; Saleh & Teich 2007). Blackbody radiation would therefore be the obvious choice for observing photon bunching, if it were not for the short coherence time associated with its spectral properties.

In a scenario where spatial coherence effects are neglected, the second order temporal correlation function for light fields can be written as

$$g^{(2)}(\tau) = 1 + |\gamma(\tau)|^2, \quad (1)$$

where  $\gamma(\tau)$  is the complex degree of coherence, or normalized self-coherence of the stationary light field with  $\gamma(0) = 1$ , which itself is proportional to the Fourier transform of the spectral density  $S(\nu)$  of the light field (Mandel & Wolf 1995). For well-defined spectral densities and coherence functions, a meaningful coherence time  $\tau_c$  can be defined, which is reciprocal to a characteristic width  $\Delta\nu$  of the spectral distribution  $S(\nu)$ .

For blackbody light sources in the optical regime, the coherence time  $\tau_c$  given by Planck's law is on the order of  $10^{-14}$  s, which is much shorter than the best time resolution  $\tau_t$  of a few  $10^{-11}$  s of existing photodetectors. As shown by (Scarl 1968), the observable excess from uncorrelated pair detections,  $g^{(2)}(\tau = 0) - 1$ , scales as  $\tau_c/\tau_t$  and is therefore only significant when the coherence time of the source is of the order of the detection time response.

Therefore, empirical observation of temporal photon

<sup>1</sup> Center for Quantum Technologies, 3 Science Drive 2, Singapore 117543

<sup>2</sup> Department of Physics, National University of Singapore, Singapore 117542

\* email: pengkian@physics.org

+ email: phyck@nus.edu.sg

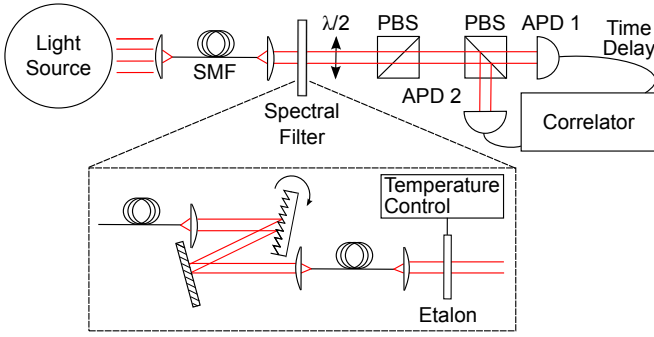


FIG. 1.— Setup to determine the temporal correlation  $g^{(2)}(\tau)$  for wideband thermal light. The initial spectrum gets filtered to a narrow optical bandwidth such that the temporal decay of the second order correlation function can be observed with conventional single photon detectors in a Hanbury-Brown-Twiss experiment. We employ a combination of a grating and a temperature-tuned etalon as a spectral filter, and ensure spatial coherence in the setup by using single mode optical fibers (SMF).

bunching from blackbody light sources has been extremely difficult, with only recent breakthroughs using two-photon absorption in semiconductors (Boitier et al. 2009), and in ghost imaging research using a narrowband Faraday anomalous dispersion optical filter (Karmakar et al. 2012; Wu et al. 2014).

In this paper, we present a spectral filtering technique that significantly increases the observed photon bunching signature from a blackbody light sources significantly, such that intensity interferometer techniques for observing celestial objects may become attractive again.

### 3. EXPERIMENT

As in previous attempts to observe photon bunching from blackbody radiation (Karmakar et al. 2012; Wu et al. 2014), we employ narrowband optical filtering of the light source in order to increase the coherence time  $\tau_c$ , and use single photon detectors with low timing uncertainties. The experimental setup is shown in Fig. 1.

First, light from different sources under investigation is coupled into a single mode optical fiber to enforce spatial coherence, because the photon bunching signature  $g^{(2)}(\tau = 0) - 1 \propto 1/M$ , where  $M$  is the number of transverse modes (Glauber 1963).

The light is then collimated with an aspheric lens and sent through the first spectral filter, which is either an interferometric bandpass filter with a full width at half maximum (FWHM) of 3 nm centered at 546.1 nm to match the  $6p7s^3S_1 - 6p6s^3P_2^0$  transition in a Hg discharge lamp, or a grating monochromator for broadband continuous spectrum. While the interference filter is sufficient to select the spectral lines of the different mercury isotopes, the grating monochromator had to be used for the blackbody sources.

The core of the monochromator is a blazed reflective diffraction grating with 1200 lines/mm mounted on a rotation stage. Light from the optical fiber (NA = 0.13) is collimated with an achromatic doublet ( $f = 30$  mm), illuminating about  $10^4$  lines of the grating. The first diffraction order is imaged with another achromat of ( $f = 30$  mm) into another single mode optical fiber. This arrangement acts as a tunable narrowband filter in the visible regime, allowing to adjust for peak emissions of blackbody light sources. A test of the transmission of

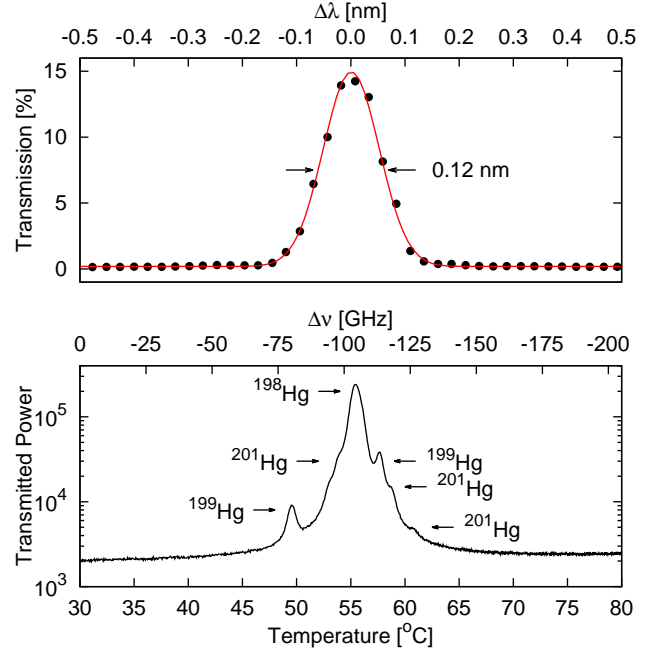


FIG. 2.— (Top) Transmission profile of grating monochromator. The solid line is a fit to a Gaussian profile to measurements for different grating angles (symbols), resulting in a full width at half maximum (FWHM) of  $0.122 \pm 0.002$  nm. (Bottom) Transmission of Hg light near 546 nm through the temperature-tuned etalon with 2 GHz bandwidth. The hyperfine structure for different isotopes is partially resolved, as identified in (Sansonetti & Veza 2010).

a narrowband laser source ( $\lambda = 532$  nm) is shown in Fig. 2 (top part). The fit to a Gaussian transmission profile leads to an optical bandwidth of  $0.122 \pm 0.002$  nm (FWHM). We typically observe a transmission of narrowband light from single mode fiber to single mode fiber of  $\approx 15\%$ .

In a second step, the light passed through a solid etalon (thickness  $d = 0.5$  mm) with flat surfaces. The etalon has a free spectral range of  $FSR = c/(2nd) = 205$  GHz, with a refractive index  $n = 1.46$  for the fused silica material (Suprasil311), and the speed of light  $c$  in vacuum. At  $\lambda = 546$  nm, the free spectral range corresponds to  $\Delta\lambda = \lambda^2/c \cdot FSR \approx 0.2$  nm so that only one transmission order should fall within the transmission width of the monochromator. Both surfaces of the etalon have dielectric coatings with a reflectivity of  $R \approx 97\%$  over a wavelength range from 390 nm to 810 nm, resulting in a transmission bandwidth (FWHM) of

$$\Delta\nu \approx FSR \cdot \frac{1-R}{\pi\sqrt{R}} \approx 2 \text{ GHz}. \quad (2)$$

The central transmission frequency of the etalon is tuned by temperature, with a scaling rate of  $-4.1$  GHz/K due to thermal expansion and temperature dependence of the refractive index. A temperature stability of  $\pm 5$  mK over the measurement duration of several hours ensures that the etalon stays on a specific wavelength. Temperature tuning allows the etalon to be always used under normal incidence, which avoids frequency walk-off (Green 1980) and spatial distortion (Park et al. 2005). To demonstrate the resolving power of this device, we tuned the peak transmission across the various spectral

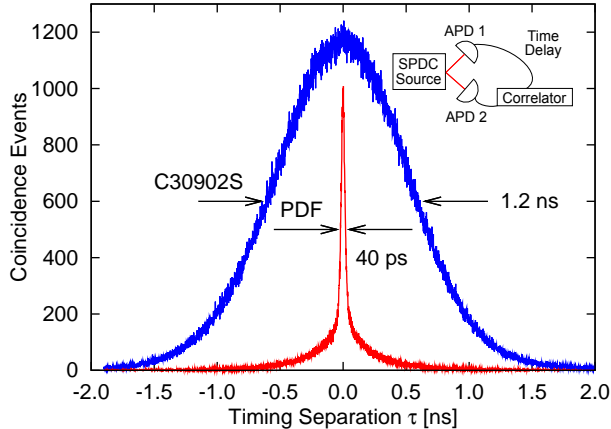


FIG. 3.— Comparison of time jitter between two actively quenched thin avalanche photodiodes (PDF), and two passively quenched deep avalanche photodiodes (C90302S) by photopair detection from light generated by spontaneous parametric down conversion (SPDC) with a coherence time below 10 ps.

lines from a Hg gas discharge lamp at 546.1 nm, revealing a partially resolved hyperfine structure for different isotopes (see Fig. 2, bottom part).

A Glan-Taylor polarizer (PBS) following the etalon selects a well-defined linear polarization mode for the photons, with the same rationale of minimizing the number of modes ending up in the temporal correlation setup. A half wave plate ( $\lambda/2$ ) transforms the polarization emerging from the grating/fiber combination such that there is maximal transmission through the PBS.

A second Glan-Taylor polarizer, rotated by  $45^\circ$  with respect to the polarization direction of the first, distributes the light onto two silicon avalanche photodiodes (APD) that provide detection time signals to a correlator. The relative orientation of the two polarizers allows to balance photodetection rates, and also helps to suppress the optical crosstalk between the two APDs due to hot carrier recombination in the devices upon detection, which would otherwise introduce false coincidence events (Kurtsiefer et al. 2001).

The temporal correlation was carried out with a digital sampling oscilloscope (4 GHz analog bandwidth, 40 Gsamples/sec, LeCroy) that can measure and histogram detection time differences between two APD events with a timing uncertainty below 10 ps.

To assess overall timing uncertainty with the detector/correlator combination, we exposed two different avalanche photodiode sets to photon pairs generated by parametric down conversion (SPDC) with a coherence time below 10 ps. The resulting temporal correlations shown in Fig. 3 reflect the overall timing resolution of the system. For APDs with a deep conversion zone (C30902S, Perkin-Elmer, passive quenching), the coincidence distribution appears roughly Gaussian, with 1.2 ns FWHM. Since the photon bunching signature  $g^{(2)}(\tau)$  of the light field under investigation needs to be convoluted with this detector response, we would observe a significant reduction of the photon bunching peak with these detectors. A second set of APDs, based on thin conversion zones (type PDF, Micro Photon Devices, active quenching) lead to a much better localized coincidence distribution with 40 ps FWHM, although a significant

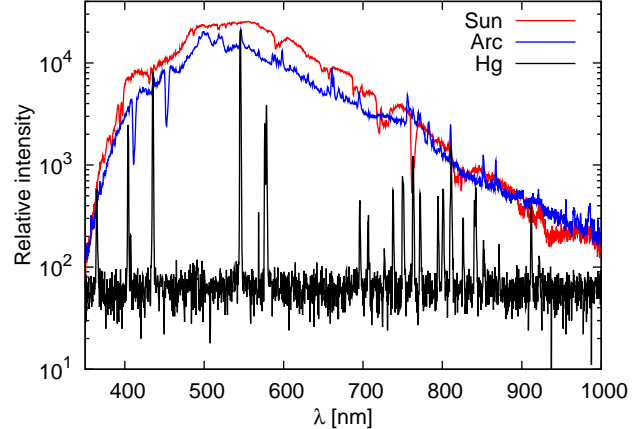


FIG. 4.— Spectrum of a Hg glow discharge lamp, an Ar arc lamp as a simulator of a stellar light source, and the Sun.

fraction of the distribution shows a tail with time differences up to 500 ps.

#### 4. RESULTS

Measurements for  $g^{(2)}(\tau)$  were performed on three light sources: a low pressure Mercury (Hg) discharge lamp as a quasi-thermal light source, a radiofrequency-driven Argon (Ar) arc discharge lamp to produce a plasma with a blackbody temperature  $\approx 6000$  K as the thermal light source, and the Sun as celestial thermal light source. Their respective spectral distributions are shown in Fig. 4. The optical filters were fixed to maximize transmission for the spectral lines around 546.1 nm in the Hg spectrum. The resulting time difference histograms are shown in Fig. 5.

To ensure proper normalization of the resulting  $g^{(2)}(\tau)$ , we independently recorded pair events with a resolution of about 300 ps with a time stamp unit that, unlike the oscilloscope, does not exhibit a significant dead time, and found that  $g^{(2)}(|\tau| \gtrsim 2 \text{ ns}) \rightarrow 1$ . To extract a meaningful set of model parameters, we assumed a Lorentzian line shape for the spectral power distribution; this is mostly to reflect the approximate transmission function of the etalon. A corresponding model function for the obtained pair rates in the histograms is

$$N(\tau) = a + b \cdot e^{-|\tau|/\tau_c} \quad (3)$$

where  $a, b$  capture the absolute event number and the degree of bunching, respectively, while  $\tau_c$  represents a coherence time. The  $g^{(2)}$  scale on the right side of diagrams in Fig. 5 is the absolute number of events, divided by fit parameter  $a$ .

For the Hg emission line at 546 nm from the low pressure glow discharge lamp, coincidence data was obtained over an integration time of 68 hours, with single detector rates of  $115000 \text{ s}^{-1}$ . The relatively large discrepancy between expected coincidences with the single rates and the observed coincidences is due to a dead time of the oscilloscope in this measurement. From the numerical fit, we find  $g^{(2)}(\tau = 0) = 1.79 \pm 0.01$  and an exponential decay with a characteristic coherence time of  $\tau_c = 0.436 \pm 0.006 \text{ ns}$ . The photon bunching signature comes very close to the expected value of 2 for a thermal state, with the difference possibly due to the residual timing

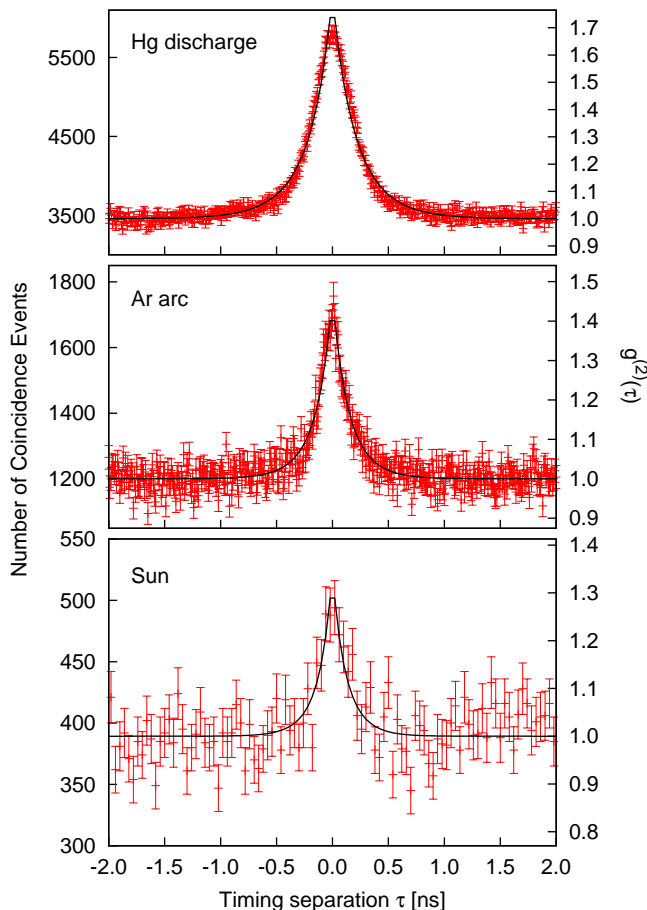


FIG. 5.— Intensity correlation function  $g^{(2)}(\tau)$  from the three thermal light sources after spectral filtering. All light sources show a significant bunching at  $\tau = 0$ , and a decay time that is well-resolved with the avalanche photodetectors. Error bars indicate uncertainties due to Poissonian counting statistics.

uncertainty of our photodetectors. While the Doppler-broadened line width for individual transitions at Hg vapour temperatures around 400 K is on the order of 235 MHz, the contribution of different hyperfine transitions from different isotopes add up to a relatively complex overall line shape of several GHz width, out of which we select a reasonable fraction with the etalon.

For the high pressure Ar arc discharge lamp, a wavelength of 540 nm was chosen to avoid contributions of a prominent peak at 546 nm, possibly caused by mercury traces in the plasma. We find  $g^{(2)}(0) = 1.45 \pm 0.03$  and a shorter coherence time  $\tau_c = 0.31 \pm 0.01$  ns with a reduced  $\chi_r^2 = 1.066$ . The wider spectrum of the cut-out blackbody radiation makes the decay time shorter, so a peak reduction due to the detector response becomes more prominent. Furthermore, residual transmission of the grating spectrometer or stray light into other transmission peaks of the etalon may contribute to light that is not coherent with the main peak on an observable time scales.

We finally collected sunlight into a single mode optical fiber with a coelostat and transferred it into the

lab. At the same working wavelength of 546.1 nm, we find  $g^{(2)}(0) = 1.3 \pm 0.1$  and a coherence time  $\tau_c = 0.26 \pm 0.05$  ns, with  $\chi_r^2 = 1.0244$  over an integration time of 45 minutes. At the moment, we do not have a good explanation what led to the reduction of the visibility of the photon anti-bunching, but seeing-induced atmospheric fluctuations in optical path length differences (Dravins 2007) may be an explanation.

## 5. SUMMARY AND OUTLOOK

We have successfully developed and demonstrated an experimental technique to resolve and explicitly measure the temporal photon bunching from thermal black-body light sources, including both discrete spectrum and blackbody spectrum such as the Sun. We observed a photon bunching signature, i.e., the excess of  $g^{(2)}(0)$  above 1, that exceeds the recently reported records of  $g^{(2)}(0) = 1.03$ , measured by (Karmakar et al. 2012), and  $g^{(2)}(0) = 1.04$ , measured by (Wu et al. 2014), by about an order of magnitude.

Compared to photon bunching observations using two-photon absorption (Boitier et al. 2009), our method would work at astronomical intensity levels, and not be constrained to cases where two photons arrive at the same detector at the same time.

We believe that with better timing control of the photodetectors and a better match of the etalon with the grating monochromator as a first stage, it should not be too technically challenging to reach the theoretical limit  $g^{(2)}(0) = 2$  for blackbody radiators.

The substantial increase in the observable photon bunching signature may reopen considerations of intensity interferometry as a useful tool in astronomical applications, where large baselines can be implemented with significantly less effort than in first order (amplitude) stellar interferometers. Current atomic clock technology should even allow the development of very large scale optical intensity interferometers with kilometer baselines, leading to micro-arcsecond resolution (Barbieri et al. 2009; Borra 2013; Dravins & LeBohec 2007; Dravins et al. 2013; Foellmi 2009; LeBohec et al. 2008; Naletto et al. 2009; Nuñez 2012; Ofir & Ribak 2006; Rou et al. 2012).

Beyond the traditional application of estimating the angular size of a celestial object via its spatial coherence length, this technique may also be used to measure photon decoherence of starlight across extended time-scales and distances, which are impossible to create in Earth-based laboratory conditions. Such experiments may e.g. provide complementary observational evidence that help to set constraints in theoretical models of quantum gravity (Lieu & Hillman 2003; Maziashvili 2009; Ng et al. 2003; Ragazzoni et al. 2003).

We acknowledge the support of this work by the National Research Foundation and the Ministry of Education in Singapore.

## REFERENCES

Asakura, T. 1970, *Opto-electronics*, 2, 115

Barbieri, C., Daniel, M. K., de Wit, W. J., et al. 2009, *Astro2010: The Astronomy and Astrophysics Decadal Survey*, 2010

- Boitier, F., Godard, A., Rosencher, E., & Fabre, C. 2009, *Nature Physics*, 5, 267
- Borra, E. F. 2013, *Monthly Notices of the Royal Astronomical Society*
- Dravins, D. 2007, *High Time Resolution Astrophysics, Astrophysics and Space Science Library* (Springer)
- Dravins, D., & LeBohec, S. 2007, *Proc. SPIE*, 6986, 698609
- Dravins, D., LeBohec, S., Jensen, H., Nuñez, P. D., & for the CTA Consortium. 2013, *Astroparticle Physics*, 43, 331, *elsevier*
- Foellmi, C. 2009, *Astronomy & Astrophysics*, 507, 1719, *eSO*
- Glauber, R. 1963, *Phys. Rev.*, 131, 2766
- Green, J. M. 1980, *J. Phys. E: Sci. Instrum.*, 13, 1302, *iOP*
- Hanbury-Brown, R., & Twiss, R. Q. 1954, *Phil. Mag.*, 45, 663
- . 1956, *Nature*, 178, 1046
- . 1957, *Proc. Roy. Soc.*, A242, 300
- Karmakar, S., Meyers, R., & Shih, Y. 2012, *Proc. SPIE*, 8518, doi:10.1117/12.929157
- Kurtsiefer, C., Zarda, P., Mayer, S., & Weinfurter, H. 2001, *J. Mod. Opt.*, 48(13), 2039
- LeBohec, S., Barbieri, C., de Wit, W.-J., et al. 2008, *Proc. SPIE*, 7013: Optical and Infrared Interferometry, doi:10.1117/12.787443, *optical and Infrared Interferometry*
- Lieu, R., & Hillman, L. W. 2003, *The Astrophysical Journal*, 585, L77
- Mandel, L., & Wolf, E. 1995, *Optical Coherence and Quantum Optics* (Cambridge University Press)
- Martienssen, W., & Spiller, E. 1964, *American Journal of Physics*, 32, doi:10.1119/1.1970023
- Maziashvili, M. 2009, *Astroparticle Physics*, 31, 344
- Millour, F. 2008, *New Astronomy Reviews*, 52, 177
- Morgan, B. L., & Mandel, L. 1966, *Physical Review Letters*, 16, 1012
- Naletto, G., Barbieri, C., Occhipinti, T., et al. 2009, *Astronomy & Astrophysics*, 508, 531, *eSO*
- Ng, Y. J., Christiansen, W. A., & van Dam, H. 2003, *The Astrophysical Journal*, 591, L87
- Nuñez, P. D. 2012, Master's thesis, University of Utah
- Ofir, A., & Ribak, E. N. 2006, *Proc. SPIE*, 6268: Advances in Stellar Interferometry, doi:10.1117/12.689123
- Park, S., Ko, H., & Park, M.-H. 2005, *Optical Engineering*, 44(4), 048001
- Ragazzoni, R., Turatto, M., & Gaessler, W. 2003, *The Astrophysical Journal*, 587, L1
- Rou, J., Nunez, P. D., Kieda, D., & LeBohec, S. 2012, *Mon. Not. R. Astron. Soc.*, 000, 1
- Saleh, B. E. A., & Teich, M. C. 2007, *Fundamentals of Photonics* (John Wiley & Sons)
- Sansonetti, C. J., & Veza, D. 2010, *J. Phys. B: At. Mol. Opt. Phys.*, 43, 205003
- Scarl, D. B. 1968, *Phys.Rev*, 175, 1661, issue 5
- Wu, L. A., Zhai, G. J., Liu, X. F., et al. 2014, *Optics Letters*